Dark solitons in dynamical lattices with the cubic-quintic nonlinearity

Aleksandra Maluckov*
Faculty of Sciences and Mathematics, University of Niš, P.O. Box 224, 18001 Niš, Serbia

Ljupčo Hadžievski
Vinča Institute of Nuclear Sciences, P.O. Box 522, 11001 Belgrade, Serbia

Boris A. Malomed
Department of Physical Electronics, School of Electrical Engineering, Faculty of Engineering, Tel Aviv University, Tel Aviv 69978, Israel
(Received 5 July 2007; published 11 October 2007)

Results of systematic studies of discrete dark solitons (DDSs) in the one-dimensional discrete nonlinear Schrödinger equation with the cubic-quintic on-site nonlinearity are reported. The model may be realized as an array of optical waveguides made of an appropriate non-Kerr material. First, regions free of the modulational instability are found for staggered and unstaggered cw states, which are then used as the background supporting DDS. Static solitons of both on-site and inter-site types are constructed. Eigenvalue spectra which determine the stability of DDSs against small perturbations are computed in a numerical form. For on-site solitons with the unstaggered background, the stability is also examined by dint of an analytical approximation, that represents the dark soliton by a single lattice site at which the field is different from cw states of two opposite signs that form the background of the DDS. Stability regions are identified for the DDSs of three types: unstaggered on-site, staggered on-site, and staggered inter-site; all unstaggered inter-site dark solitons are unstable. A remarkable feature of the model is coexistence of stable DDSs of the unstaggered and staggered types. The predicted stability is verified in direct simulations; it is found that unstable unstaggered DDSs decay, while unstable staggered ones tend to transform themselves into moving dark breathers. A possibility of setting DDS in motion is studied too. Analyzing the respective Peierls-Nabarro potential barrier, and using direct simulations, we infer that unstaggered DDSs cannot move, but their staggered counterparts can be readily set in motion.

DOI: 10.1103/PhysRevE.76.046605 PACS number(s): 05.45.Yv, 63.20.Ry, 42.65.Tg, 03.75.Lm

I. INTRODUCTION

Discrete nonlinear Schrödinger (DNLS) equations represent a vast class of dynamical lattice models [1,2] whose straightforward realizations are provided by arrays of optical waveguides (as predicted in Ref. [3], and for the first time demonstrated experimentally in Ref. [4] in a set of parallel semiconductor waveguides, see also review [5]). Optical waveguide arrays can also be created as photonic lattices in photorefractive materials [6]. Motion of solitons [7,8], interactions between them [8,9], and quasidiscrete spatiotemporal collapse [10] in DNLS systems with the Kerr (cubic) nonlinearity were studied too, theoretically and experimentally.

The DNLS model also applies to the Bose-Einstein condensate trapped in a strong optical lattice (periodic potential acting on atoms in the condensate), which was predicted theoretically [11] and confirmed in the experiment [12] (see a review of the topic in Ref. [13]). In addition to these direct physical realizations, DNLS equations may be derived, in the rotating-phase approximation, from many other nonlinear lattice models [14].

It is relevant to mention that stable discrete bright solitons were recently found also in the DNLS equation with saturable nonlinearity [15,16], which was first introduced in 1975 by Vinetskii and Kukhtarev [17]. Moreover, discrete solitons supported by the saturable self-defocusing optical nonlinearity using the photovoltaic effect were created in a waveguide array based on a photorefractive crystal [18]. The quantum DNLS equation (the Bose-Hubbard model) with the cubic-quintic nonlinearity and periodic boundary conditions was considered too [19], and few-quanta bound states were found in it.

Most studies in this field were focused on bright localized structures. However, in the course of the last several years, localized structures of the dark type have also drawn considerable interest. Publications on the latter topic were chiefly dealing with lattice models including the Kerr (cubic) nonlinearity [20]. Recently, dark solitons were experimentally observed in the defocusing lithium-niobate waveguide arrays with saturable nonlinearity [21] and their properties were studied analytically and numerically [22,23].

Thanks to the above-mentioned works, discrete solitons in the DNLS equation with the Kerr and saturable nonlinearity have been well understood. On the other hand, NLS equations with other non-Kerr nonlinearities were studied in detail mainly in continuum models. In particular, transparent media with the effective optical nonlinearity combining self-focusing cubic and self-defocusing quintic terms were demonstrated in the experiment [24]. Solitons in the NLS equation of the corresponding cubic-quintic (CQ) type are different from their counterparts in the cubic equation. The difference is salient in CQ models including a periodic potential, as shown in Ref. [25], which reported many species of stable solitons with different numbers of peaks and differ-

*maluckov@junis.ni.ac.yu

ent symmetries in the CQ NLS equation with the potential of the Kronig-Penney type (a periodic array of rectangular potential wells).

The CQ NLS equation with a very strong Kronig-Penney potential may be approximated by the DNLS equation with the CQ on-site nonlinearity. This system, which may be created as an array of waveguides built of the above-mentioned materials featuring the optical CQ nonlinearity, was introduced in Ref. [26] (the opposite limit is represented by the equation with nonlocal CQ nonlinearity [27]). In work [26], which used numerical methods and variational approximation (for DNLS equations, the latter was introduced in Ref. [28]), various families of stable bright discrete solitons were found, symmetric and asymmetric, and bifurcations linking different families were explored (strictly speaking, the DNLS equation with the CQ nonlinearity supports infinitely many coexisting stable families).

Fundamental dynamical objects supported by the CQ model are not only bright solitons, for which a well-known exact analytical solution is available [29], but also dark solitons (alias topological kink solutions) [2,30], and so-called "bubbles" [31], i.e., nontopological states maintained by nonzero boundary conditions. Analytical solutions for dark solitons are known too [29]. Studied in detail were stability conditions for static [32] and moving [33] dark solitons and bubbles in this model (standing bubbles are always unstable).

Continuing the work in these directions, it is natural to consider discrete dark solitons (DDSs) and their stability in the cubic-quintic DNLS equation, which is the subject of the present work (we do not aim to consider bubbles in this paper). It is relevant to mention that DDSs were previously considered in some other lattice models which also feature CQ nonlinearities, but of a completely different character, viz., a generalized Ablowitz-Ladik system [34], and discrete Ginzburg-Landau equations [35].

The paper is organized as follows. In Sec. II, we introduce the model and find constant-amplitude cw (continuous-wave) solutions of two types, unstaggered and staggered ones, which constitute the background supporting DDSs. An obvious necessary stability condition for DDSs is the modulational stability of the background. We identify a parameter region free of the modulational instability (MI) in Sec. III, and continue the analysis in Sec. IV, where we construct DDSs supported by both the staggered and unstaggered cw uniform states, and perform full stability analysis for them, using linearized equations for small perturbations. In either case (with the unstaggered or staggered background), DDSs further fall into two categories, viz., on-site and inter-site ones. Besides the numerical results, we also report analytical findings for the DDSs of the unstaggered on-site type, approximating it by a single lattice site between cw states of opposite signs. Despite the seemingly oversimplified nature of the analytical approach, its predictions for the stability of both unstaggered and staggered on-site DDSs turn out to be very close to numerical results. Stability regions are found for DDSs of unstaggered and staggered on-site, and staggered inter-site types, while unstaggered inter-site dark solitons are always unstable. The stability results obtained from the linearized equations are also verified by direct simulations of perturbed solitons. In Sec. V, a possibility of persistent motion of DDSs across the underlying lattice is explored by means of direct simulations, and also in a semianalytical form, in terms of the respective Peierls-Nabarro (PN) potential. Both approaches show that unstaggered DDSs cannot be set in motion, but this is quite possible for staggered ones. Section VI concludes the paper.

II. MODEL

The one-dimensional CQ DNLS equation has the form [26]

$$i\dot{\psi}_n + C(\psi_{n+1} + \psi_{n-1} - 2\psi_n) + (2|\psi_n|^2 - |\psi_n|^4)\psi_n = 0, \quad (1)$$

where ψ_n is the normalized wave function at the nth lattice site (the overdot stands for the time derivative), real constant C accounts for the inter-site coupling, and coefficients in front of the cubic and quintic terms are fixed by rescaling.

Equation (1) conserves two dynamical invariants: power (norm) $P=\Sigma_n|\psi_n|^2$, and Hamiltonian,

$$H = \sum_n \left(C\psi_n^*(\psi_{n+1} + \psi_{n-1} - 2\psi_n) + |\psi_n|^4 - \frac{1}{3}|\psi_n|^6 \right),$$

with * standing for the complex conjugate. However, these expressions diverge for dark-soliton configurations. Therefore we use *complementary norm* P_c and *complementary Hamiltonian* H_c, from which the diverging contributions, generated by the cw (continuous-wave) background, $U_\infty = \lim_{n\to\pm\infty}|\psi_n|$, are subtracted [1,2,14]:

$$P_c = \sum_n (U_\infty^2 - |\psi_n|^2), \quad (2)$$

$$H_c = \sum_n \left(C\psi_n^*(\psi_{n+1} + \psi_{n-1} - 2\psi_n) + (|\psi_n|^4 - U_\infty^4) - \frac{1}{3}(|\psi_n|^6 - U_\infty^6) \right) + P_c(2U_\infty^2 - U_\infty^4). \quad (3)$$

Equation (1) gives rise to solutions of various types. Bright localized modes (discrete solitons and breathers) were studied analytically and numerically in Ref. [26]. For the study of DDSs, the starting point is the analysis of the cw background that must support dark solitons. To this end, cw solutions to Eq. (1) are looked for as

$$\psi_n(t) = u_n e^{ikn - i\mu t},$$

where u_n is a real stationary lattice field, μ is the frequency, and $k=0$ or $k=\pi$ refers to the *unstaggered* and *staggered* stationary configuration, respectively (the corresponding solutions will be labeled by subscripts UST and ST). Accordingly, Eq. (1) gives rise to the stationary equation,

$$\mu u_n + C(u_{n+1}e^{ik} + u_{n-1}e^{-ik} - 2u_n) + 2u_n^3 - u_n^5 = 0. \quad (4)$$

cw solutions correspond to the uniform lattice field, $u_n \equiv U_\infty$, hence Eq. (4) takes the form of

$$\mu - 4C\sin^2(k/2) + 2U_\infty^2 - U_\infty^4 = 0. \quad (5)$$

Equation (5) with $k=0$ yields two unstaggered cw solutions,

$$U_\infty^2 \equiv (U_{\rm UST}^2)_{1,2} = 1 \pm \sqrt{1+\mu}. \quad (6)$$

Solution $(U_{\rm UST})_1$ exists for $\mu > -1$, while $(U_{\rm UST})_2$ is meaningful only in a finite interval, $-1 < \mu < 0$.

With $k=\pi$, Eq. (5) gives two staggered cw solutions,

$$U_\infty^2 \equiv (U_{\rm ST}^2)_{1,2} = 1 \pm \sqrt{1+\mu-4C}. \quad (7)$$

Solution $(U_{\rm ST})_1$ exists for $\mu > 4C-1$, and $(U_{\rm ST})_2$ exists in a finite interval, $4C-1 < \mu < 4C$.

III. MODULATIONAL STABILITY

Obviously, DDS solutions may not be stable unless the corresponding cw background is immune to the MI (in the cubic DNLS equation, the MI was first studied in Ref. [36]). The MI is seeded by adding infinitesimal perturbations,

$$\delta u_n = \delta u^{(0)} \exp(\Omega t + ipn), \quad (8)$$

with arbitrary real wave number p and corresponding growth rate Ω, to the cw solution:

$$\psi_n = (U_\infty e^{ikn} + \delta u_n e^{-i\kappa n}) e^{-i\mu t}, \quad (9)$$

where the perturbation may also be unstaggered ($\kappa=0$) or staggered ($\kappa=\pi$). The substitution of Eq. (9) in Eq. (1) and linearization with respect to the perturbation yield the following dispersion relations:

(i) unstaggered cw solution ($k=0$) and unstaggered perturbations ($\kappa=0$):

$$\Omega^2 = 16C \sin^2(p/2)[U_{\rm UST}^2 - U_{\rm UST}^4 - C \sin^2(p/2)]; \quad (10)$$

(ii) unstaggered cw solution ($k=0$) and staggered perturbations ($\kappa=\pi$):

$$\Omega^2 = 16C \cos^2(p/2)[U_{\rm UST}^2 - U_{\rm UST}^4 - C \cos^2(p/2)]; \quad (11)$$

(iii) staggered cw solution ($k=\pi$) and unstaggered perturbations ($\kappa=0$):

$$\Omega^2 = -16C \cos^2(p/2)[U_{\rm ST}^2 - U_{\rm ST}^4 + C \cos^2(p/2)]; \quad (12)$$

(iv) staggered cw solution ($k=\pi$) and staggered perturbations ($\kappa=\pi$):

$$\Omega^2 = -16C \sin^2(p/2)[U_{\rm ST}^2 - U_{\rm ST}^4 + C \sin^2(p/2)]. \quad (13)$$

It follows from these relations that the unstaggered background is modulationally stable (i.e., one has $\Omega^2 < 0$ at all p) for $U_{\rm UST}^2 > 1$. Therefore pursuant to Eq. (6), only the branch of the unstaggered cw solution with $(U_{\rm UST}^2)_1 = 1+\sqrt{1+\mu}$ (and $\mu > -1$) can support modulationally stable DDSs. Further, the staggered background may be modulationally stable for $U_{\rm ST}^2 < 1$. According to Eq. (7), this means that modulationally stable DDSs may be supported by the staggered cw solution with $(U_{\rm ST}^2)_2 = 1-\sqrt{1+\mu-4C}$, in the interval

$$4C - 1 < \mu < 4C. \quad (14)$$

These two possibilities, of having potentially stable DDSs with the unstaggered and staggered backgrounds, are explored in detail below. We notice that, in the case when the cw states are stable, Eqs. (10)–(13) are dispersion relations for the corresponding "phonon waves."

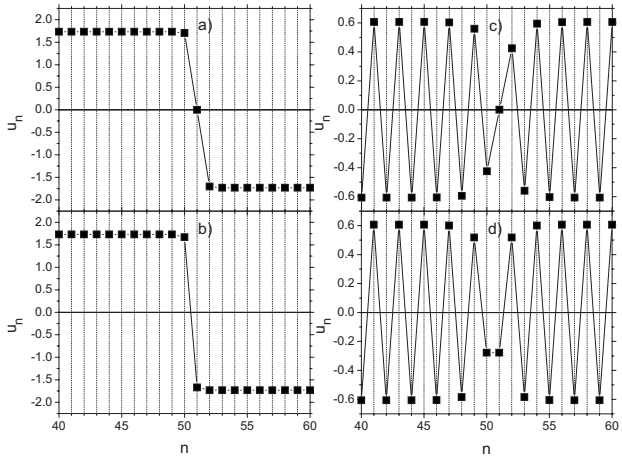

FIG. 1. Typical examples of discrete dark solitons for $C=0.4$ and $\mu=1$: (a) unstaggered on-site; (b) unstaggered inter-site; (c) staggered on-site; (d) staggered inter-site.

IV. DISCRETE DARK SOLITONS

A. General approach

With either the unstaggered or staggered background, DDS solutions of two different types can be obtained from Eq. (4): on-site, in which the sign-changing point (at which the field vanishes) coincides with a lattice site, and inter-site, in which the sign change is formally identified with a midpoint between two adjacent lattice sites. Schematically, the patterns for all four ensuing types of DDSs can be represented as $(\ldots 1,1,1,0,-1,-1,-1\ldots)$—on-site unstaggered, $(\ldots 1,1,1,-1,-1,-1\ldots)$—inter-site unstaggered, $(\ldots -1,1,-1,0,1,-1,1,\ldots)$—on-site staggered, and $(\ldots -1,1,-1,1,1,-1,1,-1\ldots)$—inter-site staggered. Examples of all four configurations for $C=0.4$ and $\mu=1$, obtained from numerical solution of Eq. (4), are presented in Fig. 1.

We examine stability of the DDSs by adapting the linear stability analysis developed in Refs. [2,20] to the present system. To this end, solutions including small perturbations, $\delta u_n \equiv \alpha_n + i\beta_n$, are looked for as

$$\psi_n = (u_n e^{ikn} + \delta u_n e^{-i\kappa n}) e^{-i\mu t}, \quad (15)$$

where u_n represents the unperturbed DDS solution, cf. expression (9) for the perturbed cw states. Then, the linearization leads to the eigenvalue problem,

$$\frac{d}{dt}\begin{bmatrix}\alpha_n \\ \beta_n\end{bmatrix} = \begin{bmatrix}0 & H^+ \\ -H^- & 0\end{bmatrix}\begin{bmatrix}\alpha_n \\ \beta_n\end{bmatrix} \equiv \mathbf{M}\begin{bmatrix}\alpha_n \\ \beta_n\end{bmatrix}, \quad (16)$$

where matrix $\mathbf{M}$ (of size $2N \times 2N$ for the lattice with N sites) is, generally, non-Hermitian. Elements of submatrices $H^\pm$ are

$$H_{ij}^+ = [(2C-\mu) - 2u_i^2 + u_i^4]\delta_{i,j} - C\cos(\kappa)(\delta_{i,j+1} - \delta_{i,j-1}),$$

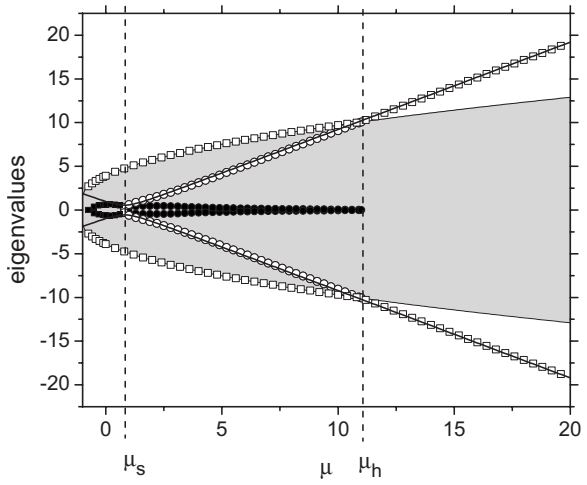

FIG. 2. The spectrum of stability eigenvalues for unstaggered on-site discrete dark solitons. Numerical results are depicted by symbols, and analytical ones, plotted as per Eq. (18), by thin black lines. The shaded region represents eigenvalues of the continuous spectrum Ω/i as given by dispersion relation (10) [recall that we consider only dark solitons supported by the modulationally stable cw background, when the continuous spectrum contains only pure imaginary eigenvalues Ω, and cannot give rise to instability, see Eq. (8)]. Empty squares correspond to stable (pure imaginary) discrete eigenvalues with the largest absolute value $|\Omega/i|$. Filled squares show pure real (unstable) eigenvalues, while empty and black circles represent, respectively, imaginary and real parts of unstable complex eigenvalues (chains of symbols which represent numerical results almost merge into bold curves). In similar plots of (in)stability spectra displayed below for dark solitons of other types, the symbols have the same meaning as here.

$$H_{ij}^{-} = -H_{ij}^{+} + 4(2u_i^2 - u_i^4)\delta_{i,j}. \tag{17}$$

Eigenvalues of matrix **M**, which determine the stability, fall into two sets. One is a continuous part of the spectrum, which arises from the background, the corresponding eigenfunctions being plane waves distorted near the core of the dark soliton. The continuous spectrum is determined by dispersion relations (10)–(13), which, for the stable background, give pure imaginary eigenvalues ($\Omega^2 < 0$) and thus cannot destabilize the DDS. A discrete part of the spectrum, which plays a crucial role in the stability analysis, is associated with the central region of the DDS. In the case when the DDS is stable, the discrete eigenvalues represent frequencies of its intrinsic modes.

B. Unstaggered dark solitons

The complete eigenvalue spectrum of matrix **M** defined in Eqs. (16) and (17) was found numerically for different values of the lattice size (N), coupling constant C, and frequency μ of the unperturbed DDS. Results for the DDS of the unstaggered on-site type are displayed in Fig. 2, for $C=0.4$. We observe that branches of discrete eigenvalues are partly embedded in the continuous spectrum [the shaded area in Fig. 2, which is precisely described by Eq. (10)]. Discrete-eigenvalue branches that do not overlap with the continuous

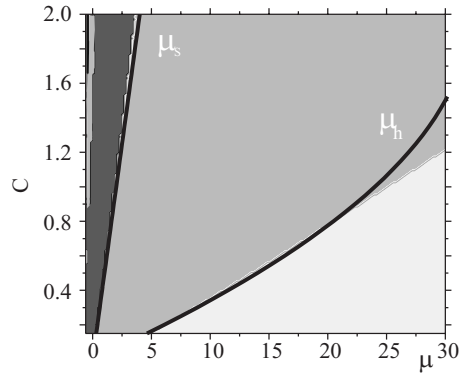

FIG. 3. Stability diagram for unstaggered on-site discrete dark solitons. Light-gray regions correspond to the pure imaginary eigenvalues (stability), gray—to complex eigenvalues (oscillatory instability), and dark-gray—to pure real eigenvalues (exponential instability). Curves depict analytical estimates of the bifurcation points μ_h and μ_s, as per Eq. (19). In stability diagrams displayed below for discrete dark solitons of other types, the gray-scale shading has the same meaning as here.

spectrum (at $\mu > \mu_h$ in Fig. 2) are pure imaginary, thus giving rise to no instability (in Fig. 2, only discrete branches with the largest imaginary eigenvalues are plotted, among those which have zero real part, i.e., are not responsible for instability). The discrete branches embedded in the continuous spectrum feature *complex* eigenvalues in region $\mu_s < \mu < \mu_h$, indicating oscillatory instability of the DDS. On the other hand, the discrete branches in the interval $-1 < \mu < \mu_s$ have *pure real* eigenvalues, which implies exponential instability of the DDS. It may be relevant to mention that the dark DDSs are, strictly speaking, marginally stable at $\mu \geq \mu_h$, as other stability is not possible in Hamiltonian systems.

The discrete branches of the spectrum can be calculated analytically if the DDS is approximated by cw solutions $\pm(U_{\mathrm{UNS}})_1$ at $n - n_c \lesseqgtr 0$, and by the phase jump at site $n = n_c$, where the amplitude vanishes:

$$u_n = \begin{cases} -(U_{\mathrm{UNS}})_1, & n > n_c, \\ u_n = 0, & n = n_c, \\ u_n = (U_{\mathrm{UNS}})_1, & n < n_c, \end{cases}$$

with $(U_{\mathrm{UNS}})_1$ given by Eq. (6) [a similar "anticontinuum," alias "anti-integrable," approximation was applied to discrete bright solitons [37]]. The substitution of this ansatz in Eq. (16) makes it possible to obtain an analytical approximation for the discrete branch,

$$\Omega_{\mathrm{discr}} \approx \pm i\sqrt{(\mu - 2C)^2 + 2C^2}. \tag{18}$$

The solid line in Fig. 2 shows that this approximation is in good agreement with the numerical results.

Decreasing the value of μ, intersection of the discrete eigenvalue branches with the continuous spectrum is identified at $\mu = \mu_h$ in Fig. 2. This gives a location of the Hamiltonian-Hopf bifurcation, i.e., the transition from the pure imaginary spectrum to that including a quartet of complex eigenvalues and remaining $2N-4$ imaginary ones. An-

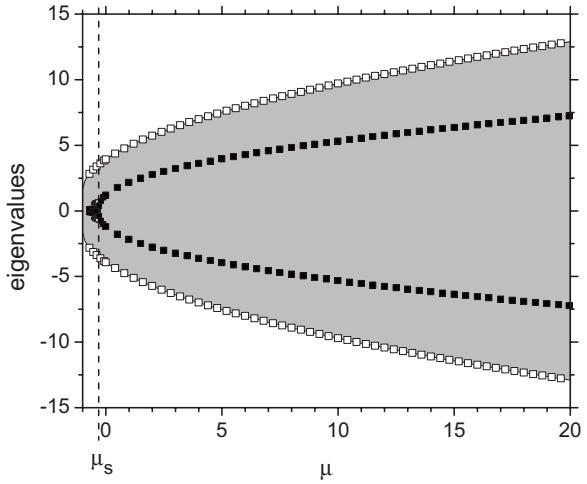

FIG. 4. The spectrum of stability eigenvalues for unstaggered inter-site dark solitons. The shaded region represents the continuous spectrum given by dispersion relation (12).

other intersection point in Fig. 2, at $\mu=\mu_s$, which follows the annihilation of the complex eigenvalues, corresponds to a saddle-center (tangential) bifurcation. It signalizes the appearance of two real eigenvalues, and approximately coincides with the minimum of the analytical curve predicted by Eq. (18). Using these facts, the bifurcation points may be approximated as follows:

$$\mu_h = 8C(4-C), \quad \mu_s = 2C. \tag{19}$$

Performing numerical calculations at many values of coupling constant C, we have generated a stability diagram in parameter plane (C,μ), as shown in Fig. 3. Light-gray regions in the figure are those with the pure imaginary spectrum, where the DDS is stable. The black lines depict analytical estimates (19), which are seen to be in good agreement with the numerical results.

The eigenvalue spectrum for DDSs of the inter-site unstaggered type is presented (for $C=0.4$) in Fig. 4, and the corresponding stability diagram in Fig. 5. In this case, the

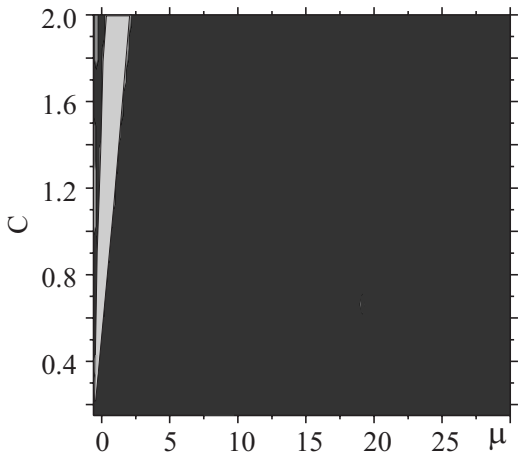

FIG. 5. The stability diagram for the unstaggered inter-site discrete dark solitons.

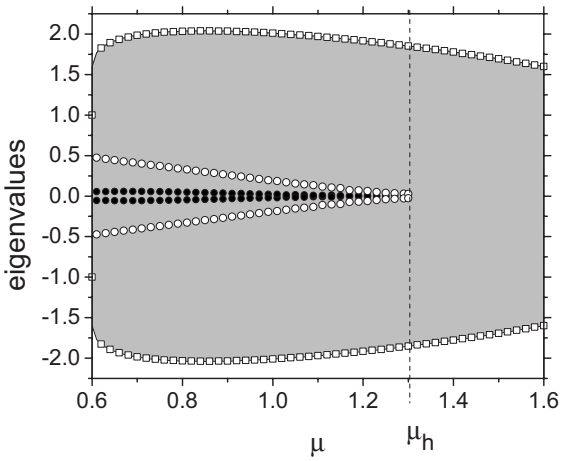

FIG. 6. The spectrum of stability eigenvalues for the staggered on-site discrete dark solitons. The shaded region represents the continuous spectrum given by dispersion relation (12).

discrete-eigenvalue branches are fully embedded in the continuous spectrum, and there are two pure real and $2N-2$ imaginary eigenvalues at all values of μ, except for a narrow region at small μ, as can be seen in Fig. 5, where a quartet of complex eigenvalues exists. Therefore the inter-site unstaggered DDS is *always unstable*. Pure real eigenvalues are created through the saddle-center bifurcation, which occurs on line $\mu=\mu_s$ in Fig. 4.

C. Staggered dark solitons

Staggered DDSs are studied in region (14), where the stable staggered background exists. The stability-eigenvalue spectrum for the staggered DDS of the on-site type, with $C=0.4$, is displayed in Fig. 6, and the respective stability diagram in Fig. 7. The discrete branches, which consist of pure imaginary or complex eigenvalues, are fully embedded in the continuous spectrum. In this case, only the bifurcation of the Hamiltonian-Hopf type occurs, at $\mu=\mu_h$. The DDS is stable

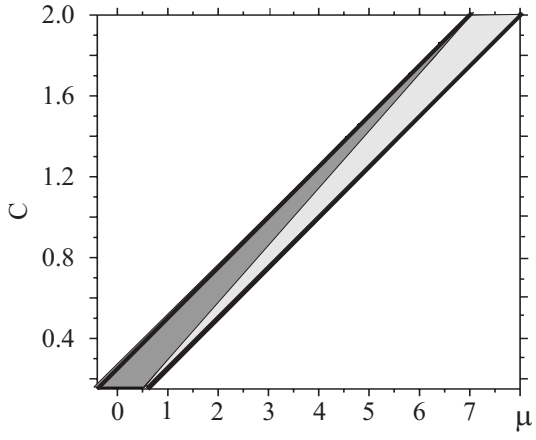

FIG. 7. The stability diagram for staggered on-site discrete dark solitons. Here and in Fig. 9 below, black lines show the stability border of the staggered background, as per Eq. (14).

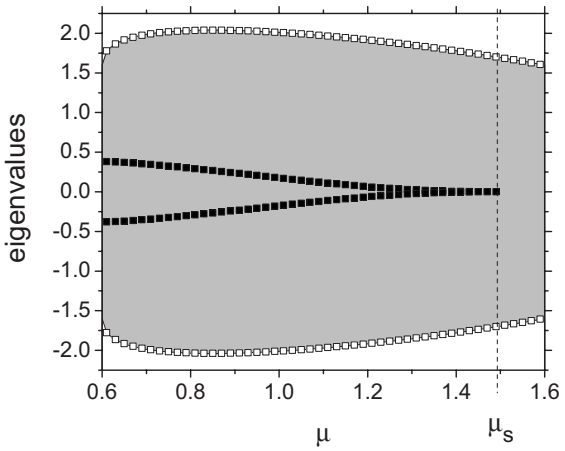

FIG. 8. The spectrum of stability eigenvalues for staggered inter-site discrete dark solitons. The shaded region represents the continuous spectrum given by dispersion relation (12).

in subinterval $\mu_h < \mu < 4C$, and unstable against oscillatory perturbations in the remaining subinterval, $4C-1 < \mu < \mu_h$, cf. Eq. (14).

The stability spectrum for the inter-site staggered DDS with $C=0.4$ is displayed in Fig. 8, and the respective stability diagram in Fig. 9. The discrete branches, which consist of pure imaginary or pure real eigenvalues, are fully embedded in the continuous spectrum. Unlike the DDS of the inter-site type supported by the unstaggered background, which are always unstable, in the present case the inter-site dark soliton is *stable* in subinterval $\mu_s < \mu < 4C$, and exponentially unstable in the remaining one, $4C-1 < \mu < \mu_s$, cf. Eq. (14).

D. Direct simulations

Direct numerical simulations have confirmed stable evolution of unstaggered and staggered DDSs in the stability regions predicted by the above analysis. With initially added perturbations, they persist as dark structures of the breather type (i.e., with some intrinsic vibrations induced by the initial perturbations), see typical examples in Fig. 10. The perturbation-induced vibrations of the stable DDSs are persistent because, as mentioned above, stable (purely imaginary) eigenvalues belonging to the discrete spectrum represent intrinsic modes of the dark solitons, that can be readily excited by the perturbation. On the other hand, when the initial unstaggered DDS is taken from a domain with complex or real eigenvalues, the instability leads to fast decay of the dark-soliton structure. Typical examples of the evolution for the unstable unstaggered DDS of the on-site (a) and inter-site (b) types are presented in Fig. 11.

Simulations of unstable staggered configurations reveal a different picture: the growth of intrinsic oscillations usually ends up with formation of a long-lived *moving* dark localized structure of a breather type. An example of the formation of

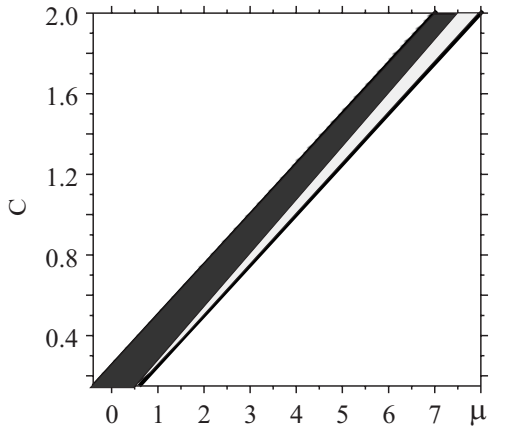

FIG. 9. The stability diagram for the staggered inter-site discrete dark solitons.

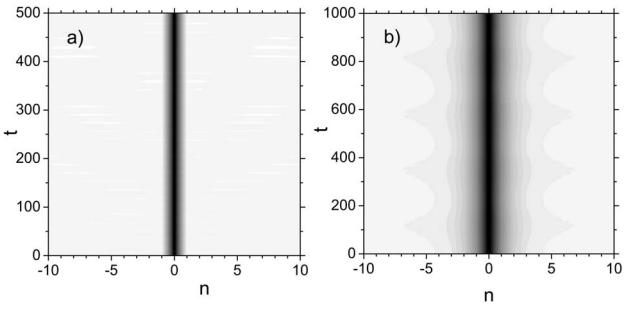

FIG. 10. Contour plots displaying evolution of perturbed dark discrete solitons, at $C=0.4$: (a) an unstaggered on-site soliton, with $\mu=16$; (b) the staggered on-site soliton with $\mu=1.35$. Both of them are robust, in accordance with the prediction of the linear-stability analysis.

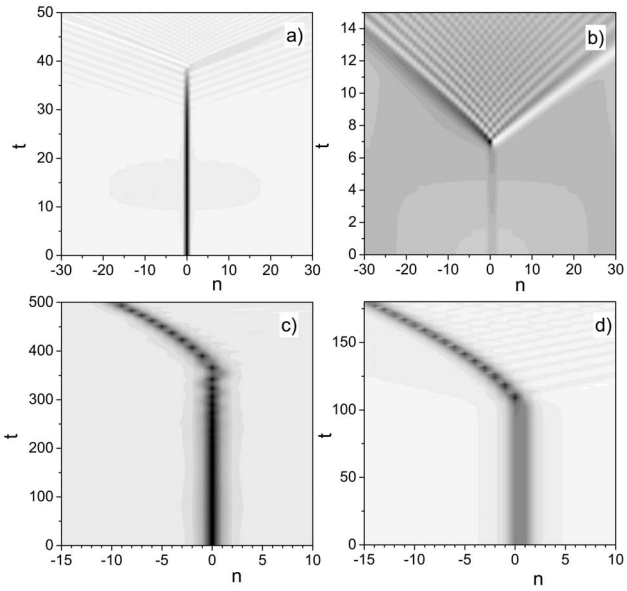

FIG. 11. Contour plots of the evolution of the perturbed dark discrete solitons for $C=0.4$: (a) the on-site unstaggered soliton with $\mu=4.3$ (destabilized by complex eigenvalues with small real parts); (b) the inter-site unstaggered soliton with $\mu=11$ (unstable due to real eigenvalues); (c) the on-site staggered soliton with $\mu=1$ (destabilized by complex eigenvalues with small real part); (d) the inter-site staggered soliton with $\mu=0.7$ (unstable due to real eigenvalues).

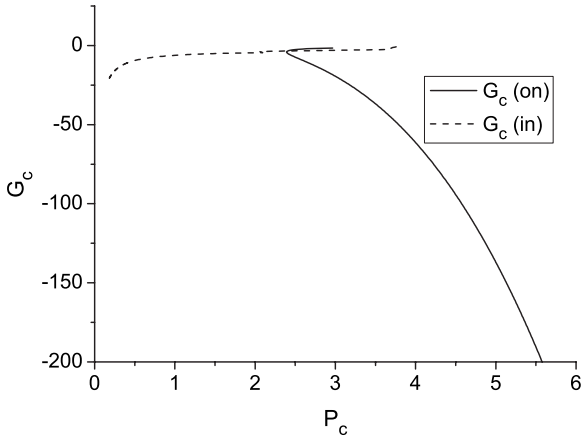

FIG. 12. The complementary (finite) free energy of unstaggered on-site and inter-site discrete dark solitons vs their complementary norms.

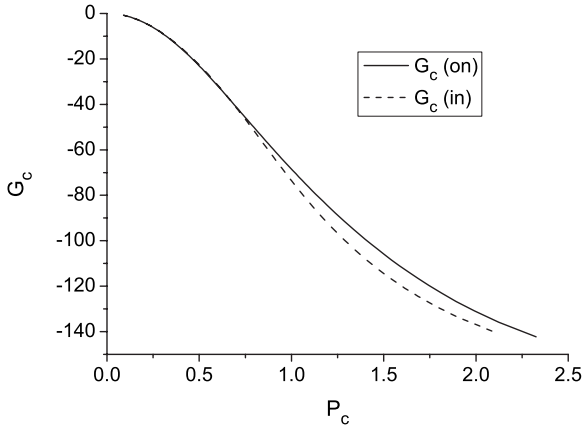

FIG. 13. The same as in Fig. 12, but for staggered discrete dark solitons.

such moving dark breathers, spontaneously created from the on-site DDS, with parameters taken in the domain with complex eigenvalues, is shown in Fig. 11(c), and a similar outcome of the evolution of an unstable inter-site DDS, with parameters picked from the domain with real eigenvalues, is presented in Fig. 11(d). The development of the oscillatory instability at the early stage of the evolution is noticeable in Fig. 11(c), which is consistent with the prediction of the linear stability analysis.

The *coexistence* of stable unstaggered and staggered DDSs in the same system is a unique feature of the discrete CQ DNLS equation. It is noteworthy too that, in Figs. 6–9, one can identify regions in parameter plane (C,μ) which *simultaneously* support stable staggered DDSs of both the on-site and inter-site types.

V. MOBILITY OF DISCRETE DARK SOLITONS

To analyze the possibility of motion of DDSs across the lattice (actually, a moving DDS will be a breather), we resort to conserved quantities P_c and H_c, defined as per Eqs. (2) and (3). Following Ref. [38], we introduce the free energy, as

$$G_c \equiv H_c - \mu P_c. \tag{20}$$

The free-energy difference between on-site and inter-site dark-soliton configurations, with equal values of norm P_c, which is

$$\Delta G_c = G_c^{(\mathrm{on})} - G_c^{(\mathrm{in})} = H_c^{(\mathrm{on})} - H_c^{(\mathrm{in})} - (\mu^{(\mathrm{on})} - \mu^{(\mathrm{in})})P_c, \tag{21}$$

determines an effective Peierls-Nabarro (PN) potential barrier, which arises from the discreteness. Dependences $G_c(P_c)$ for the unstaggered configurations of the on-site and inter-site types are displayed in Fig. 12. It is seen that the curves do not overlap, except at small μ, where DDSs are unstable. We thus conclude that the PN barrier is effectively infinite in this situation, hence free motion of stable unstaggered DDSs is *impossible*. Direct simulations (not shown here) confirm this expectation.

On the other hand, curves $G_c(P_c)$ for the staggered DDSs, as shown in Fig. 13, indicate that the PN barrier is small for the staggered solitons with a small complementary norm, which corresponds to the region in the parameter plane where stable staggered DDSs exist. This observation suggests that (quasi)free motion may be possible for stable staggered DDSs with sufficiently small P_c. This expectation is readily confirmed by direct simulations, in which staggered dark solitons were set in motion, multiplying the lattice field by $\exp(ipn)$, with a small real "kick factor" p. A typical example is displayed in Fig. 14, in which the dark soliton maintains its persistent motion, with small intrinsic vibrations.

VI. CONCLUSIONS

In this work, we have reported results of comprehensive analysis of DDSs (discrete dark solitons) in the one-dimensional lattice model with the CQ (cubic-quintic) onsite nonlinearity, which was recently introduced in Ref. [26]. First, the regions of modulational stability were found for background cw states of the unstaggered and staggered types, which may have a chance to support stable DDSs. The static solitons may be of two types, on-site and inter-site, depending on the location of their center relative to the lattice. The DDSs were constructed, and their stability against

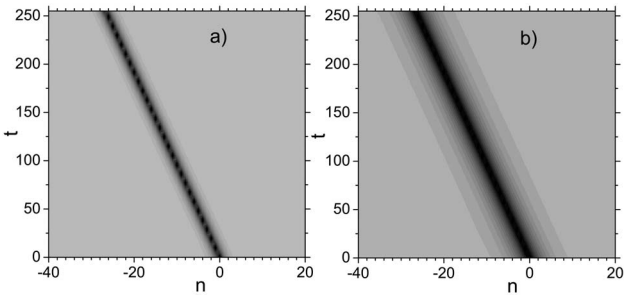

FIG. 14. Contour plots which represent persistent motion of staggered dark discrete solitons (in the form of weakly excited dark breathers): (a) $C=0.4$, $\mu=1.35$; (b) $C=0.4$, $\mu=1.56$.

small perturbations (in the framework of the linearized equation) was investigated by means of numerical methods. The stability of the on-site unstaggered DDSs was also examined with the help of the analytical approximation, that represents the on-site dark soliton by a single lattice site at which the field vanishes, being elsewhere set identical to the cw states of two opposite signs that form the background of the DDS. Stability regions for the DDSs of the on-site unstaggered, and both on-site- and inter-site staggered types, have been identified, while the inter-site unstaggered dark solitons were found to be always unstable. A noteworthy feature of the CQ model is that stable DDSs of the unstaggered and staggered types coexist in it.

The predicted stability of the DDSs was verified in direct simulations. Under the action of small perturbations, unstable unstaggered solitons decay, while unstable staggered solitons transform themselves into persistent moving dark lattice breathers. Also studied was a possibility of setting the DDS in motion across the lattice, by applying a transverse "kick" to it. Analyzing the effective PN potential, and running direct simulations, we have concluded that unstaggered DDSs are immobile, but staggered ones can be easily switched into a state of persistent motion.

The analyses reported in this paper can be extended in different directions. In particular, it may be interesting to study DDSs (in fact, vortices) in the two-dimensional DNLS equation with the CQ nonlinearity. Collisions between moving staggered DDSs (in the one-dimensional model) is another open problem. The work along these lines is currently in progress.

[1] P. G. Kevrekidis, K. Ø. Rasmussen, and A. R. Bishop, Int. J. Mod. Phys. B **15**, 2833 (2001).

[2] Yu. S. Kivshar and G. P. Agrawal, *Optical Solitons: From Fibers to Photonic Crystals* (Academic, San Diego, 2003).

[3] D. N. Christodoulides and R. I. Joseph, Opt. Lett. **13**, 794 (1988).

[4] H. S. Eisenberg, Y. Silberberg, R. Morandotti, A. R. Boyd, and J. S. Aitchison, Phys. Rev. Lett. **81**, 3383 (1998).

[5] D. N. Christodoulides, F. Lederer, and Y. Silberberg, Nature (London) **424**, 817 (2003).

[6] J. W. Fleischer, G. Bartal, O. Cohen, T. Schwartz, O. Manela, B. Freedman, M. Segev, H. Buljan, and N. K. Efremidis, Opt. Express **13**, 1780 (2005).

[7] M. J. Ablowitz, Z. H. Musslimani, and G. Biondini, Phys. Rev. E **65**, 026602 (2002).

[8] I. E. Papacharalampous, P. G. Kevrekidis, B. A. Malomed, and D. J. Frantzeskakis, Phys. Rev. E **68**, 046604 (2003).

[9] J. Meier, G. I. Stegeman, Y. Silberberg, R. Morandotti, and J. S. Aitchison, Phys. Rev. Lett. **93**, 093903 (2004); J. Meier *et al.*, Opt. Express **13**, 1797 (2005); Y. Linzon, Y. Sivan, B. Malomed, M. Zaezjev, R. Morandotti, and S. Bar-Ad, Phys. Rev. Lett. **97**, 193901 (2006).

[10] D. Cheskis, S. Bar-Ad, R. Morandotti, J. S. Aitchison, H. S. Eisenberg, Y. Silberberg, and D. Ross, Phys. Rev. Lett. **91**, 223901 (2003).

[11] A. Trombettoni and A. Smerzi, Phys. Rev. Lett. **86**, 2353 (2001); G. L. Alfimov, P. G. Kevrekidis, V. V. Konotop, and M. Salerno, Phys. Rev. E **66**, 046608 (2002); R. Carretero-González and K. Promislow, Phys. Rev. A **66**, 033610 (2002).

[12] F. S. Cataliotti, S. Burger, C. Fort, P. Maddaloni, F. Minardi, A. Trombettoni, A. Smerzi, and M. Inguscio, Science **293**, 843 (2001); M. Greiner, O. Mandel, T. Esslinger, T. W. Hänsch, and I. Bloch, Nature (London) **415**, 39 (2002).

[13] M. A. Porter, R. Carretero-González, P. G. Kevrekidis, and B. A. Malomed, Chaos **15**, 015115 (2005).

[14] S. Aubry, Physica D **103D**, 201 (1997); R. S. MacKay and S. Aubry, Nonlinearity **7**, 1623 (1994); S. Flach and C. R. Willis, Phys. Rep. **295**, 181 (1998); G. P. Tsironis, Chaos **13**, 657 (2003); D. K. Campbell, S. Flach, and Y. S. Kivshar, Phys. Today **57** (1), 43 (2004).

[15] M. Stepić, D. Kip, L. Hadžievski, and A. Maluckov, Phys. Rev. E **69**, 066618 (2004); L. Hadžievski, A. Maluckov, M. Stepić, and D. Kip, Phys. Rev. Lett. **93**, 033901 (2004).

[16] A. Khare, K. Ø. Rasmussen, M. R. Samuelsen, and A. Saxena, J. Phys. A **38**, 807 (2005).

[17] V. O. Vinetskii and N. V. Kukhtarev, Fiz. Tverd. Tela (Leningrad) **16**, 3714 (1974) [Sov. Phys. Solid State **16**, 2414 (1975)].

[18] F. Chen, M. Stepić, C. E. Ruter, D. Runde, D. Kip, V. Shandarov, O. Manela, and M. Segev, Opt. Express **13**, 4314 (2005).

[19] J. Dorignac, J. C. Eilbeck, M. Salerno, and A. C. Scott, Phys. Rev. Lett. **93**, 025504 (2004).

[20] M. Johansson and Yu. S. Kivshar, Phys. Rev. Lett. **82**, 85 (1999); R. Morandotti, H. S. Eisenberg, Y. Silberberg, M. Sorel, and J. S. Aitchison, *ibid.* **86**, 3296 (2001); D. Mandelik, R. Morandotti, J. S. Aitchison, and Y. Silberberg, *ibid.* **92**, 093904 (2004); B. Sanchez-Rey and M. Johansson, Phys. Rev. E **71**, 036627 (2005); H. Susanto and M. Johansson, *ibid.* **72**, 016605 (2005).

[21] E. Smirnov, C. E. Ruter, M. Stepic, D. Kip, and V. Shandarov, Phys. Rev. E **74**, 065601(R) (2006).

[22] E. P. Fitrakis, P. G. Kevrekidis, H. Susanto, and D. J. Frantzeskakis, Phys. Rev. E **75**, 066608 (2007).

[23] L. Hadzievski, A. Maluckov, and M. Stepic, Opt. Express **15**, 5687 (2007).

[24] F. Smektala, C. Quemard, V. Couderc, and A. Barthélémy, J. Non-Cryst. Solids **274**, 232 (2000); G. Boudebs, S. Cherukulappurath, H. Leblond, J. Troles, F. Smektala, and F. Sanchez, Opt. Commun. **219**, 427 (2003); C. Zhan, D. Zhang, D. Zhu, D. Wang, Y. Li, D. Li, Z. Lu, L. Zhao, and Y. Nie, J. Opt. Soc. Am. B **19**, 369 (2002).

[25] I. M. Merhasin, B. V. Gisin, R. Driben, and B. A. Malomed, Phys. Rev. E **71**, 016613 (2005); J. Wang, F. Ye, L. Dong, T. Cai, and Y.-P. Li, Phys. Lett. A **339**, 74 (2005).

[26] R. Carretero-González, J. D. Talley, C. Chong, and B. A. Malomed, Physica D **216**, 77 (2006).

[27] D. Mihalache, D. Mazilu, F. Lederer, L.-C. Crasovan, Y. V. Kartashov, L. Torner, and B. A. Malomed, Phys. Rev. E **74**, 066614 (2006).

[28] B. A. Malomed and M. I. Weinstein, Phys. Lett. A **220**, 91 (1996).

[29] Kh. I. Pushkarov and D. I. Pushkarov, and I. V. Tomov, Opt. Quantum Electron. **11**, 471 (1979); Rep. Math. Phys. **17**, 37 (1980); S. Cowan, R. H. Enns, S. S. Rangnekar, and S. S. Sanghera, Can. J. Phys. **64**, 311 (1986); J. Herrmann, Opt. Commun. **87**, 161 (1992).

[30] Yu. S. Kivshar and B. Luther-Davies, Phys. Rep. **298**, 81 (1998).

[31] I. V. Barashenkov and V. G. Makhankov, Phys. Lett. A **128**, 52 (1988); I. V. Barashenkov, A. D. Gocheva, V. G. Makhankov, and I. V. Puzynin, Physica D **34**, 240 (1988).

[32] D. E. Pelinovsky, Y. S. Kivshar, and V. V. Afanasjev, Phys. Rev. E **54**, 2015 (1996); S. Tanev and D. I. Pushkarov, Opt. Commun. **141**, 322 (1997); H. W. Schürmann and V. S. Serov, Phys. Rev. E **62**, 2821 (2000); D. J. Frantzeskakis, P. G. Kevrekidis, and N. P. Proukakis, Phys. Lett. A **364**, 129 (2007).

[33] I. V. Barashenkov, T. L. Boyadjiev, I. V. Puzynin, and T. Zhanlav, Phys. Lett. A **135**, 125 (1989); I. V. Barashenkov, Phys. Rev. Lett. **77**, 1193 (1996).

[34] S. González-Pérez-Sandi, J. Fujioka, and B. A. Malomed, Physica D **197**, 86 (2004).

[35] K. Maruno, A. Ankiewicz, and N. Akhmediev, Phys. Lett. A **347**, 231 (2005); C. Q. Dai and J. F. Zhang, Opt. Commun. **263**, 309 (2006).

[36] Y. S. Kivshar and M. Peyrard, Phys. Rev. A **46**, 3198 (1992).

[37] S. Aubry, Physica D **71**, 196 (1994).

[38] T. R. O. Melvin, A. R. Champneys, P. G. Kevrekidis, and J. Cuevas, Phys. Rev. Lett. **97**, 124101 (2006).